to Kipke's waveriders were used so that a proper comparison could be made. Figure 3 shows a typical correlation with some of the available experimental data. It is seen that the agreement is quite good, in particular, the viscous correction on the C_D parameter gives expecially good results. Figures 4–6 depict the influence of body geometry on the lift to drag ratio. It is seen for example, that for a given wedge angle (actually, the shock angle is what is shown), the amount of negative dihedral does not greatly effect the maximum attainable ratio of L/D. The higher (L/D) values are attained with smaller wedge angles, as one might expect. These general trends are also observed in the next two figures. In Fig. 5, L/D is plotted as a function of α. Again, the variation of $\varphi_o/2$ is not particularly significant. It is seen, for example, that β_L plays a more influencial role. Figure 6 shows L/D as a function of the lift coefficient. Again the same trends are observed. While the maximum values of L/D seem to indicate that one should seek a slender wedge with minimum dihedral, Fig. 7 shows the major drawback of this configuration. It is seen that τ, the volume parameter, varies directly with both the dihedral and wedge angles. This effect combines to give the minimum volume coefficient at the maximum (L/D) positions. It therefore, becomes apparent that a tradeoff study of $(L/D)_{max}$ as τ is required to mate a particular configuration to a given set of flight parameters.

References

[1] Love, E. S., "Manned Lifting Entry," *Astronautics and Aeronautics*, No. 5, May 1966.

[2] Trimpi, R. L., Grant, F. C. and Cohen, N. B., "Aerodynamic and Heating Problems of Advanced Reentry Vehicles," *Aerodynamic of Space Vehicles*, NASA SP-23, Dec. 1962.

[3] Eggers, A. J. and Swenson, B. L., "Lifting Entry Vehicles for Future Space Missions," *Astronautics and Aeronautics*, No. 3, March 1967.

[4] Nonweiler, T., "Delta Wings of Shapes Amenable to Exact Shock Wave Theory," *Journal of the Royal Aeronautical Society*, Vol. 67, Jan. 1963, pp. 39–40.

[5] Spence, A. and Seddon, J., "The Use of Known Flow Fields as an Approach to the Design of High Speed Aircraft," AGARD CP 30, Paper 10, *Proceedings of the AGARD Specialists' Meeting on "Hypersonic Boundary Layers and Flow Fields,"* London, England, May 1968.

[6] Squire, L. C., "Calculations of the Pressure Distribution on Lifting Conical Wings with Applications to the Off-Design Behavior of Waveriders," AGARD CP 30, Paper 11, *Proceedings of the AGARD Specialists' Meeting on "Hypersonic Boundary Layers and Flow Fields,"* London, England, May 1968.

[7] Pike, J., "Experimental Results from Three Cone Flow Waveriders," *Proceedings of the AGARD Specialists' Meeting on "Hypersonic Boundary Layers and Flow Fields,"* London, England, May 1968.

[8] Kipke, K., "Experimental Investigation of Waveriders in the Mach Number Range from 8 to 15," AGARD CP 30, Paper 13, *Proceedings of the AGARD Specialists' Meeting on "Hypersonic Boundary Layers and Flow Fields,"* London, England, May 1968.

Mach Reflection from Overexpanded Nozzle Flows

W. L. CHOW* AND I. S. CHANG†

University of Illinois at Urbana-Champaign Urbana, Ill.

FOR two-dimensional nozzle flows under highly overexpanded conditions, the shock generated from the corner at the nozzle exit cannot be regularly reflected from the centerline of symmetry and Mach reflection generally occurs. Referring to Fig. 1, where a typical Mach reflection from such a nozzle flow situation is depicted, somewhere along the straight incident weak shock I, a triple point T appears. A reflected shock R which may be weak or strong and a Mach stem (MS) which is a curved strong shock are initiated from the triple point along with a slip line S indicating the entropy discontinuity. Early studies of regular and Mach reflection of shocks were carried out by Bleakney and Taub and by Taub et al.[1–3] They were mainly concerned with transient flow cases within the shock tube. Excellent agreement has been obtained between the theoretical and experimental results for regular reflection of shocks. Experimental data also supported the three shock theories for the triple point when the incident wave is strong.

The present investigation is restricted to the study of Mach reflection associated with a steady two-dimensional overexpanded nozzle flow. The experience gained in the study of ejector flowfield[4] suggests that this problem belongs to the category of inviscid interaction between the two streams as long as the center core flow is distinct, and the viscous effects, such as prevailing along the slip-line or along the jet boundary, can only contribute to a modifying influence to the flowfield.

It is thus believed that the shock configurations as well as the accompanying flowfield including the Mach stem height can be established through the consideration that the center core flow should eventually reach a state which is equivalent to choking for a uniform one-dimensional flow. In addition, previous study of shock wave-viscous layer interaction[5] provided the evidence that the shock structure can only be modified within the rarefied flow regime, so that the Rankine-Hugoniot shock relations for air flow can be applied with confidence at the triple point when Mach reflection occurs. Perhaps it may be argued that for high nozzle Mach numbers, the flow would separate away from the corner before Mach reflection of a uniform approaching flow appears. It should be realized that under such conditions, Mach reflection with nonuniform approaching flow probably occurs within the nozzle. This situation can be studied only after the model of Mach reflection with uniform approaching flow has been developed.

The method of consideration discussed above is indeed fruitful. Some of the results obtained are reported here. Figure 2 shows the condition of occurrence of triple point configuration. Since all incident shocks are generated from the nozzle corner, the deflection angle δ_2 must be smaller than the attachment limit δ_{al} corresponding to the nozzle Mach number. δ_{rl} represents the limit for regular reflection which has been reported previously.[1] When the usual criteria of equal pressure and streamline angle across the slip-line are imposed to determine the triple point shock system, it is found that the triple point can occur only within the region bounded by the two curves labelled as δ_{n3} and δ_{n4}. δ_{n3} represents the limiting conditions when the reflected shock is "normal" whereas δ_{n4} corresponds to conditions when the Mach stem shock is "normal" at the triple point. These two curves intersect on the horizontal axis around the value of $M_1 = 1.484$ $(\gamma = 1.4)$. In addition, sonic conditions behind the reflected shock at the triple point ($M_3 =$

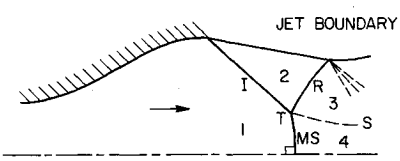

Fig. 1 Mach reflection from overexpanded nozzle flows.

Received April 5, 1972, revision received May 8, 1972. This research was carried out under the partial financial support from NASA through Research Grant NGL 14-005-140.

Index categories: Shock Waves and Detonations; Jets, Wakes, and Viscid-Inviscid Flow Interactions; and Supersonic and Hypersonic Flow.

* Professor of Mechanical Engineering, Department of Mechanical and Industried Engineering. Member AIAA.

† Graduate Research Assistant, Department of Mechanical and Industrial Engineering.

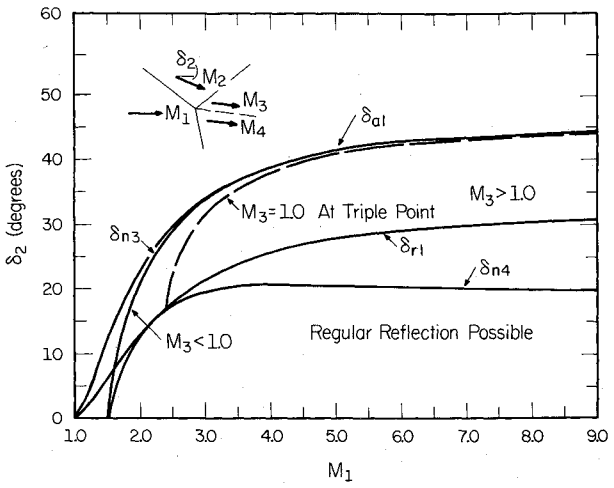

Fig. 2 Occurrence of triple point shock configuration.

1.0) are also identified. From these calculations it is believed that the Mach reflection can only occur within the region bounded by curves of δ_{n4} and δ_{n3}.

A single strip analysis of the method of integral relations[6] has been employed to calculate the flow development within both regions 3 and 4 (Ref. 7). It should be mentioned that the configuration of the slip-line is yet unknown and a step-by-step pressure-streamline angle matching across the slip-line is needed to establish its configuration as well as the strength of the reflected shock.

It is pertinent that for flow behind oblique shock waves the derivatives of flow properties including the shock strength are functions of the surface curvature at the point of shock generation. These initial flow derivatives for region 3 can be established from expressions given by Traugott[6] after modified for two-dimensional flows, by imposing vanishing stand-off distance.

Originally it appears to be extremely attractive to approximate the lower stream by a one-dimensional treatment, especially in view of the fact that the variation of entropy within the lower stream seems to be insignificant. It was found that in the early part of the flow development along the slip-line, the pressure increases and a one-dimensional calculation will be unable to match such a flow condition. To simplify the calculations, one dimensional flow analysis is introduced in conjunction with the method of characteristics for the upper supersonic flow after the flows along the slip-line are in states of acceleration. Entropy gradients have also been sweepingly ignored within these parts of the flowfields. It is also necessary to introduce the expansion fan into the flowfield which results from the reflection of the curved shock from the freejet boundary. These calculations may be continued until the lower sIream reaches the sonic state. For a fixed nozzle height, the correct Mach stem height is the one which causes the sonic lower stream occurring at a section of minimum area (choking criterion). Figure 3 shows a flow pattern associated with such Mach reflection calculations. In practice, the Mach stem height may be fixed and the insertion

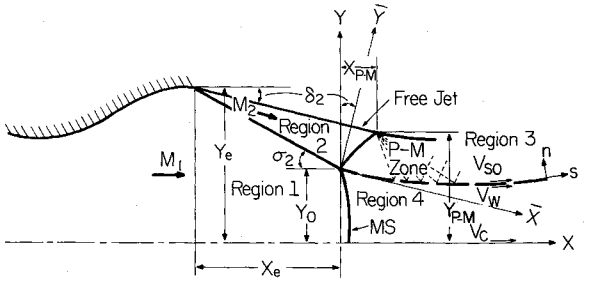

Fig. 3 Illustration of detailed flowfield with Mach reflection.

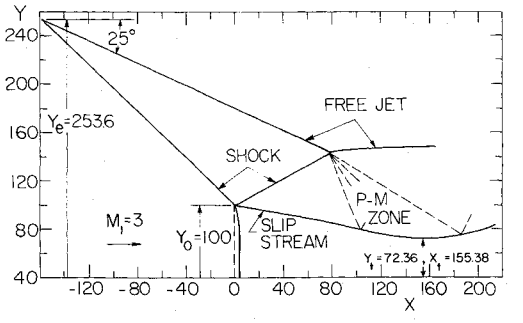

Fig. 4 Mach reflection configuration ($M_1 = 3.0$, $\delta_2 = 25°$).

of the Prandtl-Meyer expansion at the correct location would readily allow the evaluation of the corresponding nozzle height under this particular operating condition. Figures 4 and 5 show the in-scale plot of the established flow configurations of $M_1 = 3$ at two values of the incident shock strength. It is interesting to observe the difference in these flow patterns. Figure 6 shows variations of flow properties within regions 3 and 4 from such calculations. Finally, Fig. 7 shows the variation of Mach stem height for different Mach numbers under conditions of different pressure ratios. It is also interesting to point out that Mach reflection pattern has also been established when δ_2 is below the regular reflection limit.

Additional investigation for initially subsonic flows behind the reflected shock ($M_3 < 1.0$) at the triple point is being carried out. It is strongly believed that the appearance of Mach disk within the axially symmetric flowfield is governed by the same flow interaction phenomena. In addition, the present analysis should be improved by incorporating the effect of vorticity and more detailed description of the Mach stem configuration. Further effort is needed to identify the pressure ratio which separates the Mach reflection regime and the strong curved shock regime of the nozzle flows.

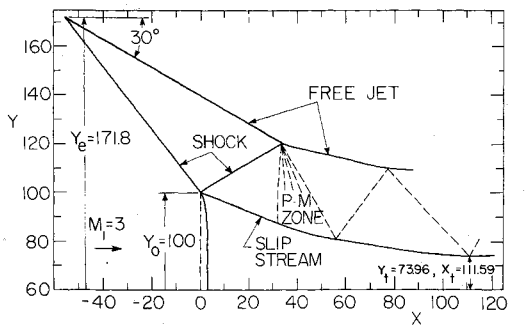

Fig. 5 Mach reflection configuration ($M_1 = 3.0$, $\delta_2 = 30°$).

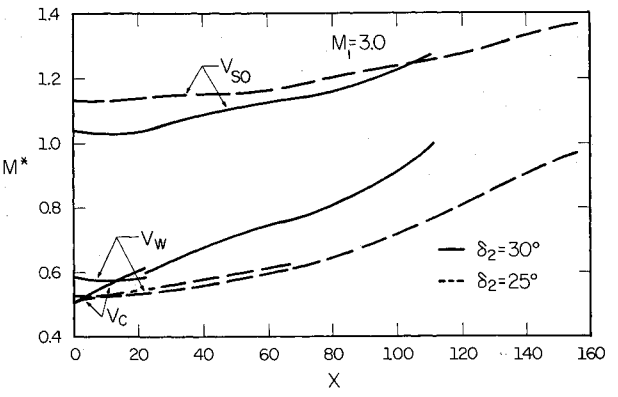

Fig. 6 Velocity variations associated with flow with Mach reflection.

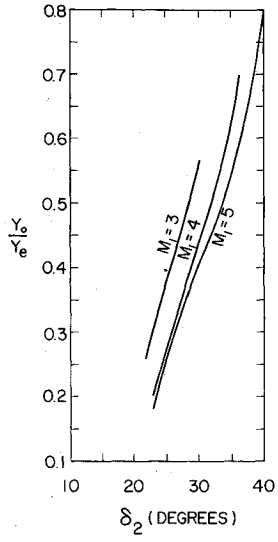

Fig. 7 Height of Mach stem.

References

[1] Bleakney, W. and Taub, A. H., "Interaction of Shock Waves," *Reviews of Modern Physics*, Vol. 21, No. 4, Oct. 1969, pp. 584–605.

[2] Taub, A. H., "Singularities on Shock," *American Mathematical Monthly*, No. 7, Pt. II, 1954, p. 61.

[3] Clutterham, D. R. and Taub, A. H., "Numerical Results on the Shock-Configuration in Mach Reflection," *Proceedings of the Symposium in Applied Mathematics*, Vol. VI, 1953.

[4] Chow, W. L. and Addy, A. L., "Interaction between Primary and Secondary Streams of Supersonic Ejector Systems and Their Performance Characteristics," *AIAA Journal*, Vol. 2, No. 4, April, 1964, p. 686.

[5] Chow, W. L., "Hypersonic Rarefied Flow Past the Sharp Leading Edge of a Flat Plate," *AIAA Journal*, Vol. 5, No. 9, Sept. 1967, p. 1549.

[6] Traugott, S. C., "An Approximate Solution of the Direct Supersonic Blunt-Body Problem for Arbitrary Axisymmetric Shapes," *Journal of the Aerospace Sciences*, Vol. 27, 1960, pp. 361–370.

[7] Howlett, L. D., "A Study of Nozzle Flow Problems by the Method of Integral Relations," Ph. D. thesis, Dept. of Mechanical and Industrial Engineering, Univ. of Illinois at Urbana-Champaign, Urbana, Ill.

Errata

Errata: "Roots of the Cylindrical Shell Characteristic Equation for Harmonic Circumferential Edge Loading"

P. SEIDE

University of Southern California, Los Angeles, Calif.

[AIAAJ. **8**, 452–454 (1970)]

IN the aforementional paper[1] various versions of the cylindrical shell characteristic equation for harmonic circumferential edge-loading were solved numerically and the roots compared. It has been brought to the author's attention[1] that the coefficients of the complete Flügge equation are incorrect. The required changes are that Eqs. (3b) and (3c) should be rewritten as

Received April 12, 1972.

Table 1 Values of the roots of the complete Flügge characteristic equation for edge-loaded cylindrical shells

n	p_{n1}	q_{n1}	p_{n2}	q_{n2}
0	4.04809	4.08501	...	...
2	4.56863	3.63890	0.45591	0.37916
4	6.13012	2.98441	2.02105	1.03738
6	8.05787	2.63703	3.94978	1.38578
8	10.04291	2.44489	5.93561	1.57873
10	12.03906	2.32061	7.93266	1.70390
12	14.03797	2.23082	9.93260	1.79469
14	16.03758	2.16084	11.93343	1.86580
16	18.03728	2.10326	13.93454	1.92464
18	20.03686	2.05395	15.93577	1.97532
20	22.03626	2.01043	17.93705	2.02032
22	24.03546	1.97111	19.93838	2.06120
24	26.03445	1.93492	21.93977	2.09901
26	28.03322	1.90113	23.94123	2.13448
28	30.03178	1.96919	25.94280	2.16811
30	32.03012	1.83870	27.94447	2.20029
32	34.02824	1.80934	29.94628	2.23129
34	36.02613	1.78088	31.94824	2.26132
36	38.02378	1.75310	33.95038	2.29057
38	40.02119	1.72585	35.95270	2.31915
40	42.01835	1.69897	37.95522	2.34718
42	44.01524	1.67233	39.95797	2.37473
44	46.01184	1.64581	41.96096	2.40187
46	48.00816	1.61931	43.96421	2.42868
48	50.00416	1.59272	45.96774	2.45518
50	51.99984	1.56593	47.97156	2.48143
52	53.99519	1.53884	49.97570	2.50746
54	55.99017	1.51134	51.98018	2.53330
56	57.98479	1.48332	53.98501	2.55899
58	59.97901	1.45466	55.99021	2.58454
60	61.97281	1.42524	57.99582	2.60998
62	63.96619	1.39492	60.00183	2.63534
64	65.95912	1.36355	62.00829	2.66064
66	67.95158	1.33097	64.01520	2.68589
68	69.94354	1.29698	66.02260	2.71113
70	71.93499	1.26138	68.03050	2.73636
72	73.92590	1.22392	70.03893	2.76163
74	75.91626	1.18431	72.04790	2.78694
76	77.90603	1.14223	74.05745	2.81233
78	79.89521	1.09724	76.06759	2.83782
80	81.88376	1.04886	78.07836	2.86344
82	83.87166	0.99644	80.08976	2.88922
84	85.85889	0.93915	82.10182	2.91520
86	87.84544	0.87586	84.11457	2.94142
88	89.83128	0.80497	86.12802	2.96790
90	91.81639	0.72403	88.14219	2.99470
92	93.80076	0.62893	90.15710	3.02186
94	95.78438	0.51150	92.17275	3.04943
96	97.76724	0.34948	94.18917	3.07746
98[a]	99.59688	99.90177	96.20635	3.10602
100[a]	101.31252	102.14876	98.22430	3.13516

[a] The complete Flügge equation yields two pairs of real roots, the magnitudes of which are tabulated as p_{n1} and q_{n1}.

$$\alpha_2 = 4 + [(11 - 3\nu)/2]k + 9[(1 - \nu)/2]k^2 \quad (3b)$$

$$\alpha_3 = 6 + 3(2 - \nu)k - \nu^2 k^2 \quad (3c)$$

The roots of the various equations were recalculated for R/h of 10, 20, and 50 and n varying from 1 to 300 with the use of a double-precision polynomial root extraction routine DPRBM.[2] The corrected results for the complete Flügge equation for n varying by steps of 2 from 0 to 100 and $R/h = 10$ are shown in Table 1. Some additional results for $R/h = 10$ and $n = 150$, 200, 250, 300 are given for all three characteristic equations in Table 1a. Figure 1 is corrected as shown.

The corrected results indicate that the roots of the complete and simplified Flügge equations are in good agreement over a much larger range of n than was previously found. In both cases the pattern of the roots shifts from all complex roots to four real roots and four complex roots for large n. The value of n at